Electronic Supplementary Information (ESI)

Metal ions responsive nanochannel by H_2S absorbed in Metal-Organic Framework-based micropipette

Shiyi Tan,[ab] Chenglong Liang,[b] Yue Zhu,[b] Nannan Liu,*[abc] Jinzheng Zhang,[ab] Tingyan Ye,[ab] Kangyan Yi,[ab] Xingxing Tang [d] and Qian Shi*[b]

[a] Key Laboratory of Carbon Materials of Zhejiang Province, College of Chemistry & Materials Engineering, Wenzhou University, Wenzhou 325027, P. R. China.
[b] College of Chemistry and Materials Engineering, Wenzhou University, Wenzhou 325000, P. R. China.
[c] Institute of New Materials & Industry Technology, Wenzhou University, Wenzhou 325000, P. R. China.
[d] College of optoelectronic manufacturing, Zhejiang Industry & Trade Vocational College, Wenzhou, 325003, China

*To whom correspondence should be addressed: liunannan@wzu.edu.cn, shiq@wzu.edu.cn

Table of Content

1. Materials and reagents

All reagents are purchased and used directly without further purification. p-Phthalic acid (PTA 99%), N,N-Dimethylformamide (DMF AR 99.5%), Isopropyl Alcohol (99.8%), Ethanol absolute (99.8%), Copper nitrate trihydrate (99%), Potassium chloride (99.5%), Mercury solution (analytical standard), Zinc nitrate hexahydrate (99%), Lead nitrate (99%) was purchased from Shanghai Aladdin Biochemical Technology Co., Ltd. Indium nitrate hydrate ($InNO_3 \cdot xH_2O$ 99.9%) was purchased from Sarne Chemistry Technology (Shanghai) Co., Ltd. Acetonitrile (99.8%) was purchased from Shanghai Macklin Biochemical Co., Ltd. 1,3,5-Benzenetricarboxylic acid (99%), 3-(Triethoxysilyl) propylsuccinic anhydride (TESP-SA 95%) was purchased from J&K Chemical Ltd.

Ag/AgCl electrodes (0.50*37 mm) are purchased from Shanghai YueCi Electronic Technology Co., Ltd. Borosilicate glass (10 cm length, outer diameter: 1.2 mm, inner diameter: 0.60 mm) are purchased from Sutter Instrument Co., U.S.A.

2. Parameters of preparation for glass micropipettes.

HEAT	PULL	VEL	TIME
645	5	5	150
645	5	5	150
645	5	5	150
645	40	5	150
645	60	5	150

Table 1. Parameters of preparation for glass micropipettes. The borosilicate glass was fixed on the P-97 micropipette puller, and the glass micropipettes with fixed radius can be prepared by adjusting the parameters.

3. SEM and Microscopic photograph.

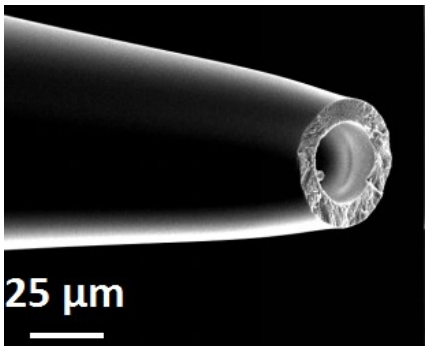

Fig. S1 SEM image of blank glass micropipette with diameter is 20 ± 1 µm.

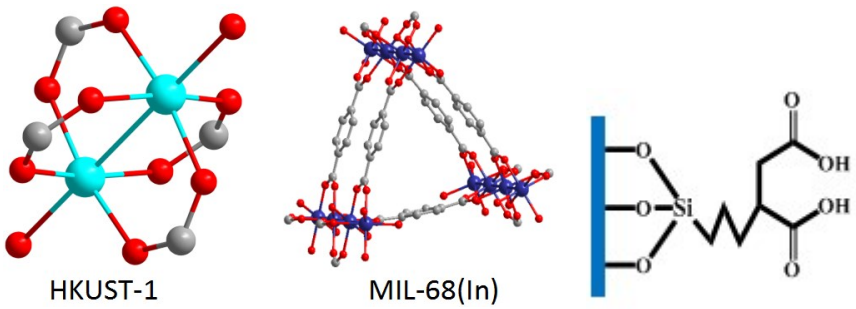

Fig. S2 After the inner surface modification of the glass micropipette, the carboxyl groups exist on the inner surface of the glass micropipette, which promotes the *in-suit* growth of MOFs in the micropipette.

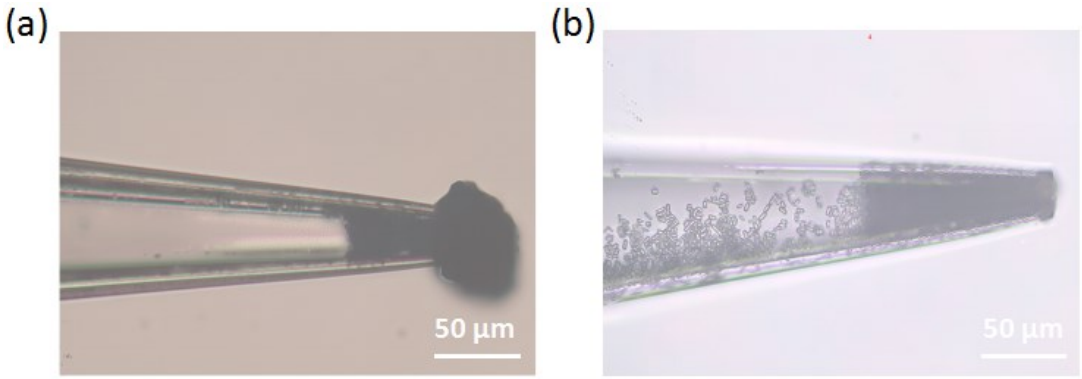

Fig. S3 Microscopic photographs of HKUST-1-MP (a) and MIL-68(In)-MP (b).

4. Current measurement after absorbing H_2S.

HKUST-1-MP and MIL-68(In)-MP were used to absorb H_2S for 10 hours, and the I-V curves were tested respectively.

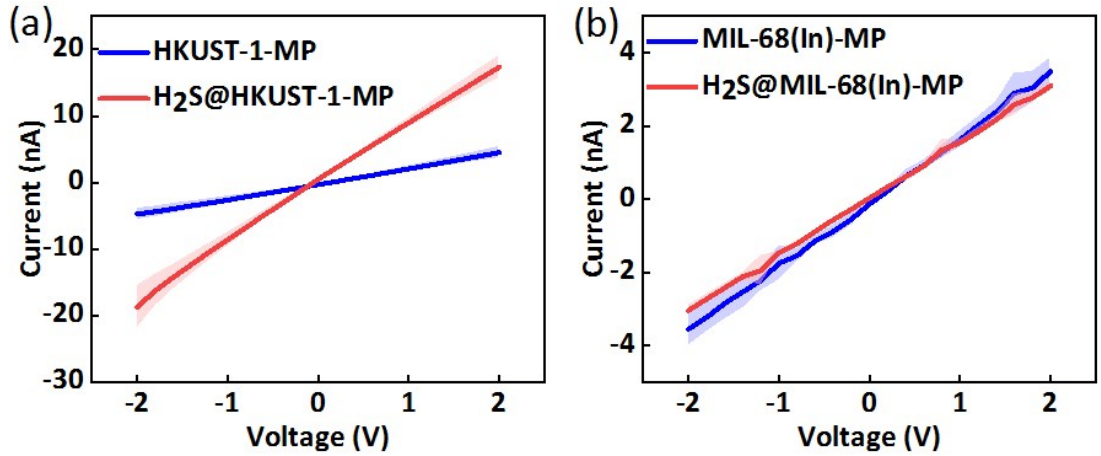

Fig. S4 (a) I-V curves in 0.1 M KCl of HKUST-1-MP and H_2S@HKUST-1-MP. (b) I-V curves in 0.1 M KCl of MIL-68(In)-MP and H_2S@MIL-68(In)-MP. The shaded area is the margin of error.

5. Current measurement of H_2S@MIL-68(In)-MP respond to Zn^{2+}.

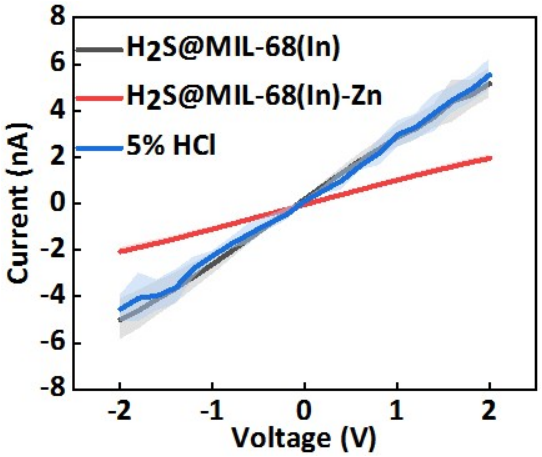

Fig. S5 I-V curves in 0.1M KCl of H_2S@MIL-68(In)-MP and after treated with 0.5 μM Zn^{2+} solution. The current returns to initial current after 5 % HCl treatment. The shaded area is the margin of error.

6. Energy Dispersive X-Ray spectroscopy (EDS) pattern.

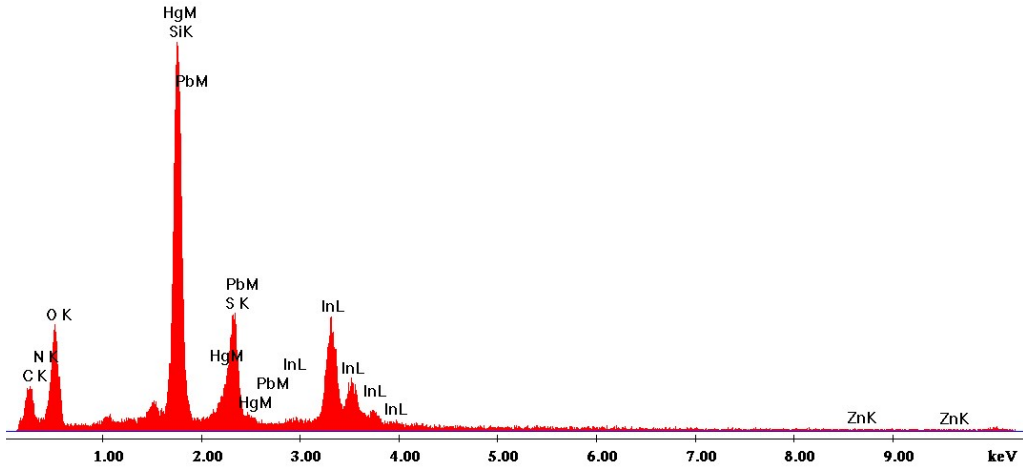

Fig. S6 Energy Dispersive X-Ray Spectroscopy of H_2S@MIL-68(In)-MP after treating with a mixture of mercury, lead and zinc ions solution.

Elem	Wt%	At%
C	2.30	4.68
N	8.52	14.88
O	34.04	52.04
Si	22.03	19.18
S	5.47	4.17
In	17.44	3.71
Hg	5.07	0.62
Pb	4.74	0.56
Zn	0.41	0.15
Total	100.00	100.00

Table 2. The contents and percentages of various elements of EDS shown.

7. XPS patterns.

The S 2p spectra analyses of the H_2S@MIL-68(In) and after treatment with mixed ions solution were shown. The peaks located at 162.98 and 161.88 eV after treatment. The peak of 162.98 eV was attributed to S_2^{2-}. The peak of 161.88 eV was attributed to the S^{2-} because of H_2S and the formation of HgS, PbS and ZnS.[1] After soaking in the mixed ions solution, the peak of S_2^{2-} shifted to the direction of decreasing the binding energy. This indicates that more sulfur and metal ions precipitate, resulting in sulfur gaining electrons and increasing electron density. Compared to H_2S@MIL-68(In), the binding energy of the peak decreases.

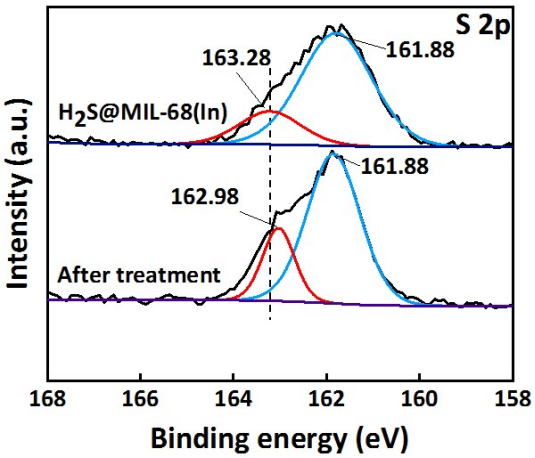

Fig. S7 The S 2p XPS spectra of the H_2S@MIL-68(In) and after treating with 5×10^4 nM mixed ions solution.

8. Current measurement of H_2S@MIL-68(In)-MP respond to Hg^{2+}.

The prepared MIL-68(In)-MP was measured with 0.1M KCl, and then used to absorb H_2S for 10 hours. After the absorption of H_2S (H_2S@MIL-68(In)-MP), the tip of H_2S@MIL-68(In)-MP was placed in 0.5 μM mercury solution for 30 minutes. After taking it out, the current of H_2S@MIL-68(In)-MP combining with mercury ions was detected. Fig. S8a shows that the H_2S@MIL-68(In)-MP sensitively responds to mercury ions and the rate of current decrease was 87%, while the MIL-68(In)-MP was only 15% (Fig. S8b). Below this threshold, the signal may stem from some non-specific interactions.

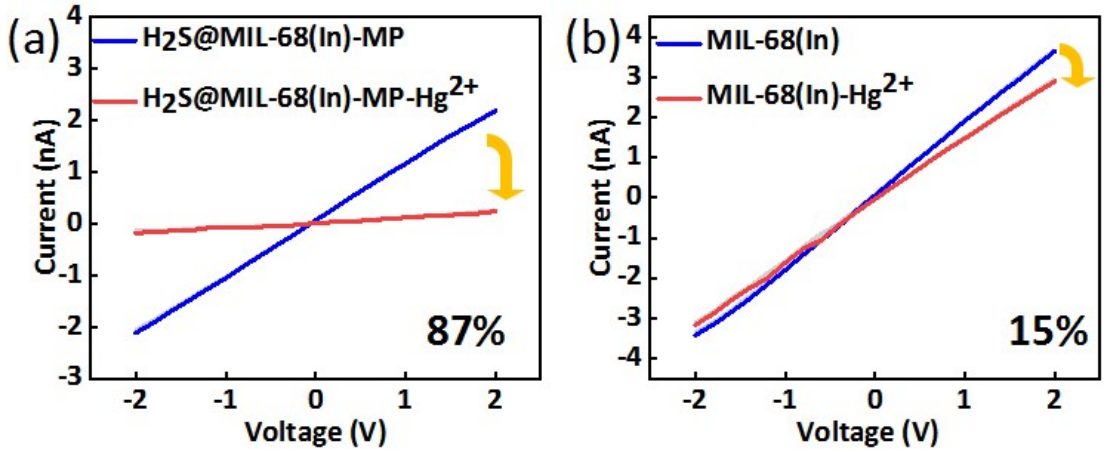

Fig. S8 I-V curves of MIL-68(In)-MP and H_2S@MIL-68(In)-MP after treated with 0.5 μM Hg^{2+} solution.

1 mM Na_2S acts as a recoverable agent for the nanochannel. Stability and reversible switching properties were further tested based on this property. However, due to the alkaline nature of the Na_2S solution, the stability of the MIL-68(In) was challenged during this process. In the first time, the H_2S@MIL-68(In)-MP was used to detect 0.5 nM Hg^{2+} which the rate of current decrease was 25.88%. The current increased 16.81% compared with the initial current when the nanochannel was opened by Na_2S. This indicates that alkaline Na_2S has a slight destructive effect on the MIL-68(In) which were modified at the tip of micropipette. In the second time, H_2S@MIL-68(In)-MP was used to detect 0.5 nM Hg^{2+}, the rate of current decrease was 26.64%, which prove that H_2S@MIL-68(In)-MP still has the ability to detect mercury. However, compared with the initial current, the rate of current decrease was only 14.30%, which was lower than rate of non-specific interactions (15%).

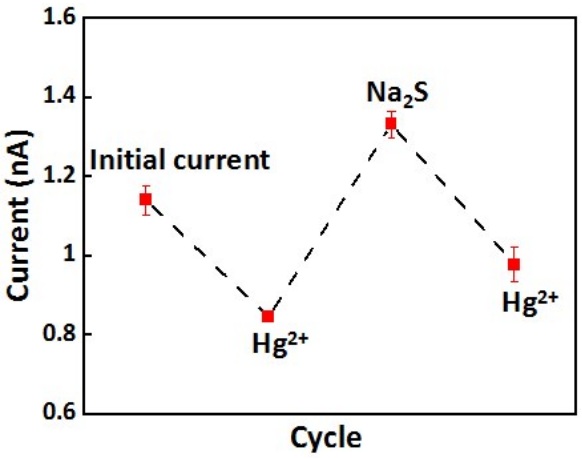

Fig. S9 The cycle performance of Hg^{2+} at the detection limit of 0.5 nM.

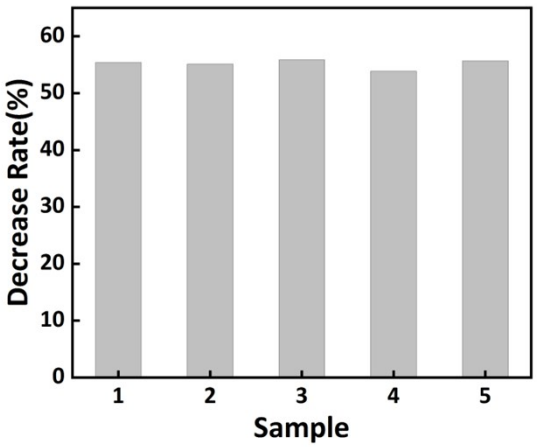

Fig. S10 Current decrease rate of H_2S@MIL-68(In)-MP bound with 0.5 μM Hg^{2+} after absorbing H_2S for 10 hours and leave for 36 hours. All signals decrease by about 55 %, which is down from 87 % in the previous test.

9. X-ray diffraction (XRD) pattern.

Both HKUST-1 and MIL-68(In) powders were dried before X-ray diffraction (XRD) analysis. The instrument used for XRD analysis is Germany Bruker D8 X-ray diffractometer. Cu Kα radiation source was used (λ = 1.5 Å). The analysis was operated at 40 mA and 40 kV, and the 2θ was varied from 5.0 to 50° with a step of 1.0°/min. By comparing the following crystal standard spectra, it was confirmed that HKUST-1 and MIL-68(In) were synthesized in the experiment.

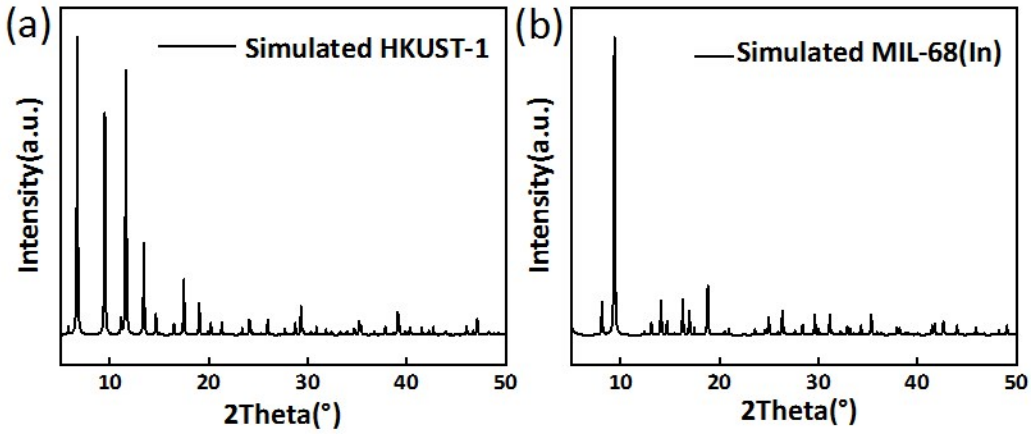

Fig. S11 XRD pattern of simulated HKUST-1 and MIL-68(In).

10. N_2 absorption isotherms of MIL-68(In) and H_2S@MIL-68(In).

Compared the N_2 absorption isotherms of MIL-68(In) and H_2S@MIL-68(In), the N_2 absorption volume of H_2S@MIL -68 (In) was 92.73cm^3/g higher than that of MIL-68(In). This may be due to the chemical reaction between MIL-68(In) and H_2S. In particular, before the N_2 absorption isotherms test, the H_2S@MIL-68(In) were activated for 10 hours at 100 °C, which may have exacerbated the reaction and caused the change of N_2 absorption behavior. Pore size distribution of MIL-68(In) and H_2S@MIL-68(In) show that most pore are still at the sizes of 2-6 nm.

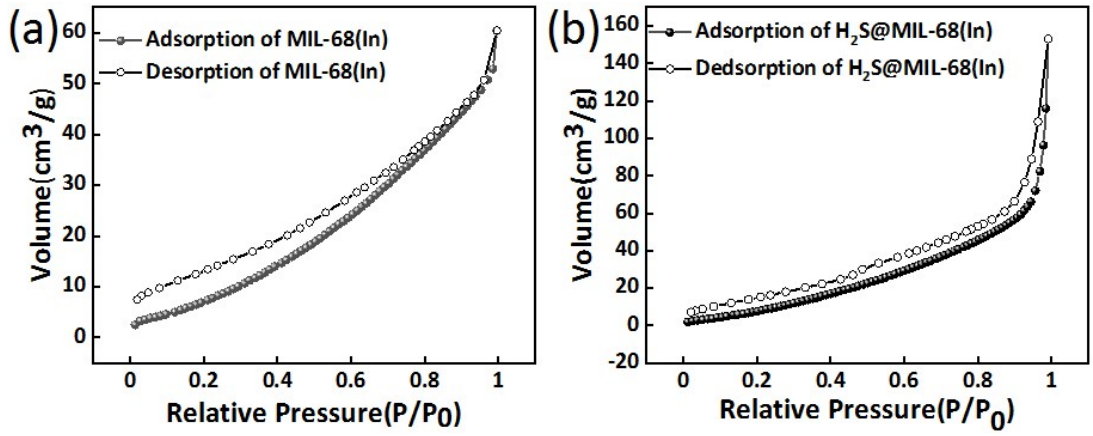

Fig. S12 N_2 absorption isotherms of MIL-68(In) and H_2S@MIL-68(In).

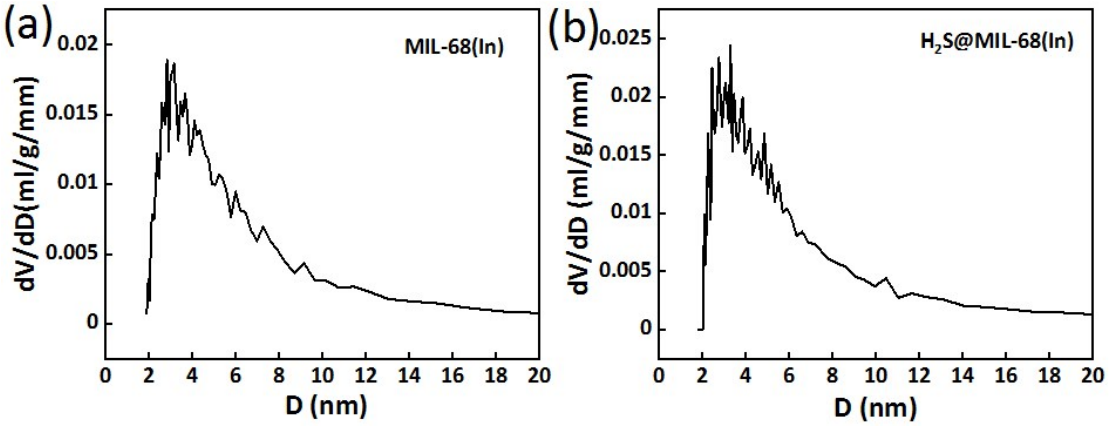

Fig. S13 Pore size distributions of MIL-68(In) and H_2S@MIL-68(In).

11. Current measuring device.

All I-V tests were performed using the following apparatus, which using two Ag/AgCl electrodes. One electrode was directly immersed in the 0.1 M KCl electrolyte, another electrode was inserted into the micropipette from the base. Keithley 6487 picoammeter (Keithley Instruments, Cleveland, OH, USA) was connected to form a closed circuit. Before the test, the electrodes were soaked overnight in sodium hypochlorite solution.

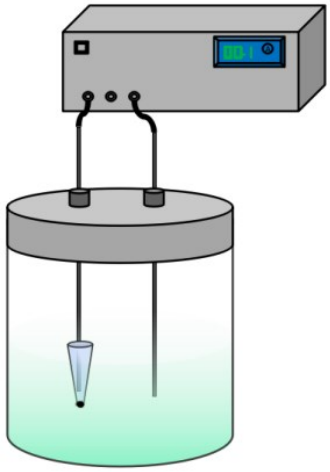

Fig. S14 Device diagram for testing the current through the micropipettes.

12. SEM of H_2S@MIL-68(In) powder combine with Hg^{2+}.

The prepared H_2S@MIL-68(In) powder was added to 0.5 μM mercury solution for soaking 30 minutes, then centrifuged and dried at 80 °C. The powder was characterized by SEM. Fig. S15 confirmed that many flocculent precipitates appear in MIL-68(In) crystals after binding with mercury.

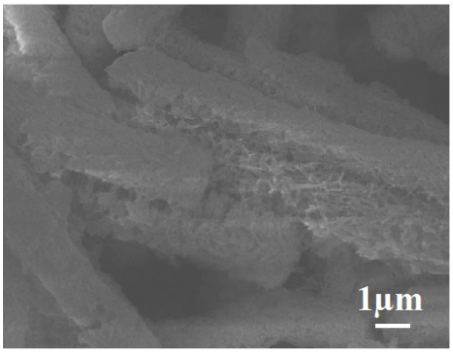

Fig. S15 SEM image of H_2S@MIL-68(In) powder combine with 0.5 μM Hg^{2+}.

13. Comparison with other sensor.

Reference	Materials	Detection Technique	Detection Limit
2	PET and AIE property organics	fluorescence and ion current signal	1 μM
3	AAO and DNA	ion current signal	1 nM
4	DNA and Fe_3O_4@Au magnetic nanoparticles	Square wave voltammograms	1.7 nM
This work	Glass micropipets and MOFs	ion current signal	0.5 nM

Table 3. Comparison of different sensors used for mercury detection.

References

1. Z. Yang, H. Li, C. Liao, J. Zhao, S. Feng, P. Li, X. Liu, J. Yang and K. Shih, *ACS Appl. Nano Mater*, 2018, **1**, 4726-4736.

2. X. Xu, R. Hou, P. Gao, M. Miao, X. Lou, B. Liu and F. Xia, *Anal. Chem.*, 2016, **88**, 2386-2391.

3. H. Wang, S. Hou, Q. Wang, Z. Wang, F. Xia and J. Zhan, *J. Mater. Chem. B*, 2015, **3**, 1699.

4. P. Miao, Y. Tang and L. Wang, *ACS Appl. Mater. Interfaces*, 2017, **9**, 3940-3947.